BNL--39349

DE87 006745

In-situ shearing interferometry of National Synchrotron Light Source mirrors

Shi-nan Qian,* Harvey Rarback, Deming Shu**

National Synchrotron Light Source, Brookhaven National Laboratory, Upton, NY 11973-5000

and

Peter Z. Takacs

Instrumentation Division, Brookhaven National Laboratory, Upton, NY 11973-5000

Abstract

In situ mirror distortion measurements were made with a lateral shearing interferometer on three mirrors in beam line X17T at the National Synchrotron Light Source. Lateral shearing interference is insensitive to vibrational motion in five of the six degrees of freedom, so it is well-suited for investigations in the synchrotron radiation (SR) environment. No distortion was seen in an uncooled silicon carbide mirror and in a cooled copper alloy mirror on X17TB, but a change in the radius of an uncooled electroless nickel-plated aluminum cylinder mirror of about 6.2% was observed on X17TA. Angular vibrations in the 2-3 arc second range were easily observed on one of the beam lines, as was an overall mirror rotation in the arc second range.

Introduction

The application of synchrotron radiation to scientific and technical problems has expanded rapidly over recent years. A large number of SR storage rings, each with many beam lines, are currently in operation or are in the development stage throughout the world. The performance of high-brightness sources is presently limited by the optical quality of beam line optics. One of the limiting factors in system performance is the in situ response of individual optical components in the SR environment. Prior to installation into the beam line, each component is usually characterized for figure and finish in the metrology laboratory. But after installation into the beam line, we have had no way of monitoring the real-time performance of individual components, other than indirect inference from complete system performance degradation. What happens to an optical surface under actual SR irradiation? Does the optical element respond to thermal effects according to model predictions? These questions are of interest for optics exposed to the SR environment for the following reasons:

(a) The temperature distribution in optical components and mounting mechanisms changes significantly because of power absorbed from the beam, resulting in changes in the direction and quality of the reflected wavefront;

(b) The absorbed power distribution on the optical surface is not uniform, resulting in local surface deformations and changes in the intensity distribution within the beam;

(c) Vibrations from the vacuum system, cooling system, motors and general floor activity are transmitted to the optical mounts.

We know these effects are important in beam degradation on some beam lines at the NSLS. We observe that the image point on the sample moves around as a result of component vibration in addition to inherent electron beam instabilities; the size of the image varies as a result of thermal distortion of optical components; measured intensity fluctuates because of component vibration. We report here the first efforts to measure the in-situ performance of three "first" mirrors in NSLS beam line X17 using shearing interferometry.

Interferometry is a traditional and sensitive method for testing optical components. But the usual Twyman-Green and Fizeau interferometers, which require separate reference surfaces, are not suited for use in SR beam lines for the following reasons: (a) System vibration is so great that interference fringes are nearly impossible to see and record; (b) If the interferometer is used outside of the vacuum enclosure, the poor quality of the window port will make interpretation of the interferogram very difficult. The main advantages of using shearing interferometry on SR beam lines are: (a) It is a very simple technique, the main element used is a single solid shearing plate; (b) Interference fringes are produced by reflection of the test wavefront from the two surfaces of a solid shearing plate. The fringes are insensitive to motions produced by vibrations in five of the six degrees of freedom, and the long-term stability of the system has proved to be excellent; (c) It is a self-referencing method, in that the wavefront under test provides its own reference wavefront. No special remote reference surface is required and, hence, there are no differential vibrations between the sheared wavefronts which can make recording the

interferogram difficult; (d) It is quite easy to interpret differential measurements made with the shearing interferometer, which lends itself to making the thermal distortion measurements induced by exposure to the x-ray beam.

Principle and equipment

The lateral shearing interferometer is used in this experiment.[1] The principle of operation is shown in Fig 1: a shearing plate of finite thickness reflects a wavefront from its front and back surfaces, producing two nearly colinear wavefronts with a lateral displacement. The interference fringes occur in the region of overlap between the two wavefronts. If the incident wavefront changes, the spacing and direction of the shearing fringes will change. The sensitivity to changes in the incident wavefront depends on the shearing quantity determined by the thickness and refractive index of the plate, and on the angle of incidence, wavelength and the amount of overlap. For plane wavefronts, if M is the number of fringes within the shearing overlap region of length S, the difference in slope, $d\alpha$, between the two sheared wavefronts is

$$d\alpha = \frac{\lambda M}{2S} \tag{1}$$

If we are interested only in changes in the wavefront slope between two successive measurements, assuming that $\Delta M = 0.2$ can be easily identified by eye and for S = 20 mm, then a sensitivity of $d\alpha = 0.6$ arc seconds or a surface height difference of 0.06 microns can be achieved. In the case of spherical wavefronts, the situation occurring in the x-z plane in the beam propagating toward the observation plane is illustrated in Fig. 2. The shape of a surface of constant phase in each circular wavefront is given by the parabolic approximation:

$$Z(x) = \frac{x^2}{2R} \tag{2}$$

$$Z(x-s) = \frac{(x-s)^2}{2R}$$

The optical path difference (OPD) between the wavefronts in the region of overlap is given by:

$$OPD(x) = Z(x) - Z(x-s) = \frac{xs}{R} - \frac{s^2}{2R} \tag{3}$$

where R is the radius of curvature of the propagating wavefront. What we measure in the interferogram is the <u>difference</u> in the OPD between two points, x_1 and x_2, measured in terms of fringes, each fringe being an increment of one wavelength in this geometry.

$$OPD(x_2) - OPD(x_1) = M\lambda = \frac{S}{R}(x_2 - x_1) \tag{4}$$

The direct measurable quantities in Eq. (4) are M, S, and (x_2-x_1), so we can easily determine the absolute radius of curvature of the wavefront by measuring fringes in the interferogram. But what we are really after are <u>changes</u> in R over a period of time manifested by a change in M, the number of fringes in a constant distance interval. Taking differentials in Eq. (4) we are led to the result

$$dR = \frac{-R^2\lambda}{S\ \Delta x}\, dM \tag{5}$$

For the case of the cylinder mirror on X17TA, R = 287 m and S = Δx = 41 mm, we calculate that the sensitivity of radius change to fringe number is 31 meters per fringe. Since fringe shifts on the order of 0.1 fringe are easily measurable, the technique is sensitive to a change in the radius of about 1% in this case.

A diagram of the lateral shearing interferometer optical system is shown in Fig. 3. The beam from a He-Ne laser is incident on a spatial filter assembly and a collimator lens, which function as a beam expander. The collimated beam passes through the shearing plate and the mirror box window, is reflected from the test mirror, returns to the shearing plate which then shears the wavefront laterally in the plane of the paper. This is the horizontal shearing condition. We can also rotate the shearing plate to produce vertical shearing fringes. Photographic film was placed in the region of the interference to record the interference pattern.

Mirror distortion experiment

Horizontal shearing interferometer measurements were made on the first mirrors of the two branch lines on the X17T mini-undulator beam line.[2] The measurement parameters are summarized in Table I. The X17TB mirror is a thin solid CVD SiC slab with a flat surface with no active cooling provision. No distortion was seen in this mirror in two different runs with two different undulator gaps and power loadings. The temperature rise was measured by a thermocouple attached to the back surface of the mirror. The result was to be expected because of the excellent thermal conductivity and thermal expansion properties of the SiC. This actually represents a worst-case test for the shearing interferometer, since the expected distortion was negligible.

The X17TA mirror is an electroless nickel plated aluminum substrate figured as a segment of a cylinder, oriented with the cylinder axis in the vertical direction. No provision for external cooling is available for this mirror, and no temperature measuring devices were attached to the mirror so that the temperature of the mirror was not known. The curvature of the wavefront incident on the mirror was adjusted by slightly defocusing the collimating lens to approximately match the curvature of the cylinder in the horizontal plane. Photographs of the fringe patterns were taken at various time intervals before and during the irradiation cycle, and the data was analyzed according to the situation shown in Fig. 3 and the analysis in an earlier section of this paper. Typical interferogram curves are shown in Fig. 4 for the cases of before irradiation and after 3 hours. Several marks (not easily seen on the reproductions) indicate a constant distance in the image plane, facilitating the measurement of the change in fringe number. For the ENP/Al mirror, the fringe number changed by -0.58 from the initial 10 fringes over the constant distance interval. One calculates from Eq. (5) that the change in radius of the mirror is 18 meters for a fractional change in radius of 6.2% at the end of the 3 hour period. This change in radius is equivalent to a maximum slope error of 3.6 arc seconds from the original cylindrical surfaces, which number can be used to estimate the amount of degradation at the focus of the beam or in the throughput of a crystal monochromator. From the earlier sensitivity calculation, one should be able to detect changes in slope on the order of 0.5 arc seconds on mirrors with radii in the range of several hundred meters.

Measurements were also attempted on a third mirror which replaced the temporary SiC mirror on X17TB. This mirror is an actively-cooled copper alloy substrate with a plano polished electroless nickel surface, which is designed to withstand the higher power densities anticipated from the soft x-ray undulator to be installed on beam line X1 at the NSLS. Owing to a shortage of time, only one distortion measurement was made, and no distortion of the plano surface was seen at the relatively low power levels afforded by the X17T mini-undulator.

TABLE 1. MIRROR DISTORTION MEASUREMENTS

	X-17TB		X-17TA
Mirror Dimensions (mm)	180 × 50 × 8		180 × 70 × 40
Mirror Radius	∞		287 m
Mirror Material	SiC		ENP/Al
Shearing Plate Dimensions (mm)	50.8 × 25.4 × 25.4		ϕ300 × 55
Shearing Angle	45°		45°
Shearing Quantity, S	18.9 mm		41.0 mm
Mirror Temperature Variation	12.5°C	24.4°C	?
Undulator Gap	42.8 mm	33.3 mm	46.7 mm
Storage Ring Current	83 ma	77 ma	128 ma
Number of Fringes Observed, M	5	5	10.0
Change in Fringe Number, dM	<0.1	<0.1	-0.58
Change in Radius, ΔR	--	--	+18 m
$\frac{\Delta R}{R}$			+6.2%

Mirror vibration measurement

As mentioned above lateral shearing interferometry is insensitive to vibration in all but one angular degree of freedom about an axis normal to the plane of shear. We distinguish between two types of vibration: high frequency vibrations that serve to smear out dark fringes, making them appear fuzzy to the eye, and low frequency vibrations with

periods of minutes or hours, which are equivalent to an overall rotation of the surface. Rotation of the interferometer platform as a possible source of the low frequency vibration was eliminated because the rotation was observed to be a function of exposure of the test mirror to the SR beam and was reversible upon removal of the incident beam. Table II summarizes the vibration results. Both horizontal and vertical shear was used on the SiC mirror on X17TB, while only the horizontal shear configuration was used on X17TA. The relationship used to convert fringe shift, dM, to rotation angle, $d\alpha$, is

$$d\alpha = - \frac{\sqrt{n^2-\sin^2\alpha}}{T \sin 2\alpha} \lambda \, dM \qquad (6)$$

where n is the refractive index, T is the plate thickness and α is the angle of incidence. The mounting system for the SiC mirror was not optimized to provide a stable configuration: it was a temporary configuration which was replaced by a permanent mirror and mounting system after these measurements were made. The vibration results show that this mounting configuration had serious vibration problems which were confirmed by the experimenters attempting to use the unstable beam reflected off of the mirror. This measurement of instability in the mirror mounting system can be used to separate effects of beam motion due to optical system instability from those effects due to inherent electron beam orbit instabilites. The mounting mechanism on X17TA is much more stable than that on X17TB as evidenced by the smaller magnitude of the high frequency vibration. One sees, however, that the low frequency rotation of the X17TA mirror is rather large in the horizontal plane. This is most likely the result of the non-uniform distribution of SR flux across the surface of the mirror. In fact, about one-half to two-thirds of the incident flux is intercepted by the side of the mirror and the mount closest to the source, rather than being spread across the figured surface. This probably heats up one side of the mirror more than the other, resulting in an apparent rotation of the surface caused by a differential thermal expansion along the 180 mm length. A finite element analysis of this case has not been performed, so we cannot confirm this conjecture.

TABLE 2. MIRROR VIBRATION MEASUREMENTS

			X-17TB	X-17TA
Shearing Plate Thickness		H	25.4 mm	55.0 mm
		V	3.0 mm	-
Shearing Angle		H	45°	45°
		V	45°	-
High Frequency Angle Vibration	Fringe Number	H	0.7	<0.1
		V	0.14	-
	Rotation Angle ($d\alpha$)	H	2.0 arc sec	0.13 arc sec
		V	3.3 arc sec	-
Slow Angle Vibration	Fringe Number	H	<.05	1.7
		V	-0.1	-
	Rotation Angle ($d\alpha$)	H	-	2.2 arc sec
		V	1.65 arc sec	-

Conclusions

Our initial attempts at measuring mirror distortions produced by SR undulator beam power loading have demonstrated the feasibility of shearing interferometry for in-situ SR applications. The lateral shearing interferometer is quite rugged, insensitive to most vibrations, is stable over long time periods, and requires minimal alignment and adjustment. The results of the measurement can be interpreted very simply. The system can easily be used for remote monitoring in inaccessible areas, such as behind radiation shield walls, with the addition of a video camera system because of its long-term stability and freedom from adjustment. It has proven to be a useful tool in separating out image motion caused by optical component vibration from that caused by electron beam instabilities. It can be used to confirm distortion predictions from finite-element structural calculations. The specific shearing geometry can be tailored to optimize the sensitivity to a particular feature, such as a localized bump on the surface or an overall curvature change.

Acknowledgments

The authors would like to thank Manfred Grindel, President, Continental Optical Corporation, for loaning us the large shearing plate used in this investigation and for several useful discussions. We also thank Dr. Wolfgang Eberhard, Exxon Corporation, for his cooperation and assistance in making the measurements on X17TA.

This research was supported by the U. S. Department of Energy under Contract No. DE-AC02-76CH00016.

References

*Shi-Nan Qian, Visiting Scientist from the University of Science and Technology of China, Hefei, Anhui, People's Republic of China.

**Deming Shu, Visiting Scientist from the Institute of High Energy Physics, Academia Sinica, Beijing, People's Republic of China.

1. For a review of shearing interferometry, see Chapter 4, "Lateral Shearing Interferometers" by M. V. R. K. Murty in Optical Shop Testing, Daniel Malacara, ed., (Wiley, New York, 1978).

2. Jacobsen, C. and Rarback, H., "Predictions on the Performance of the Soft X-Ray Undulator," Proc. SPIE 582, 201-212 (1986).

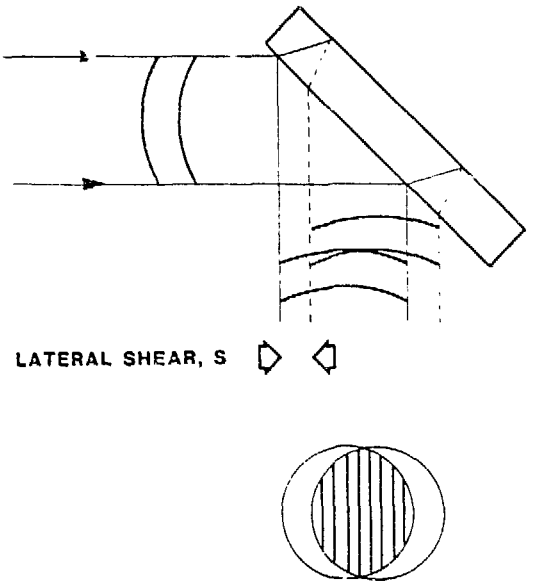

Fig. 1

Principle of the lateral shearing interferometer. A wavefront incident from the left is reflected from the front and rear surfaces of a thick parallel plate which produces two identical wavefronts displaced laterally with respect to each other. The interferogram is recorded in the region of overlap. The interference pattern produced by an ideal spherical wavefront is indicated in the lower part of the figure.

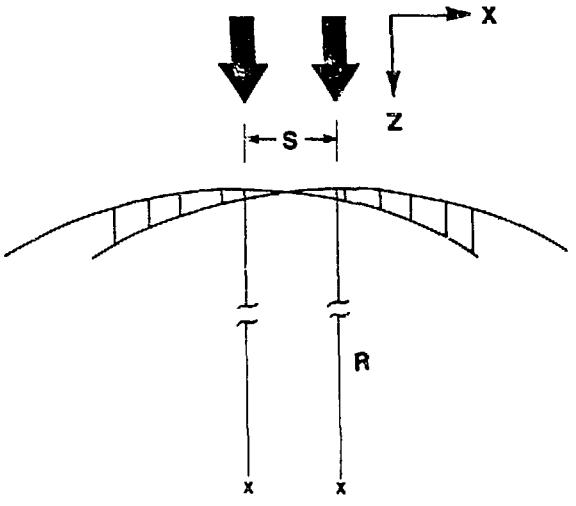

Fig. 2

The OPD at each point in the x-direction in the frame is related to the shear distance, S, and the radius of curvature of the wavefront, R. Spherical wavefronts produce a linear fringe pattern with uniform spacing.

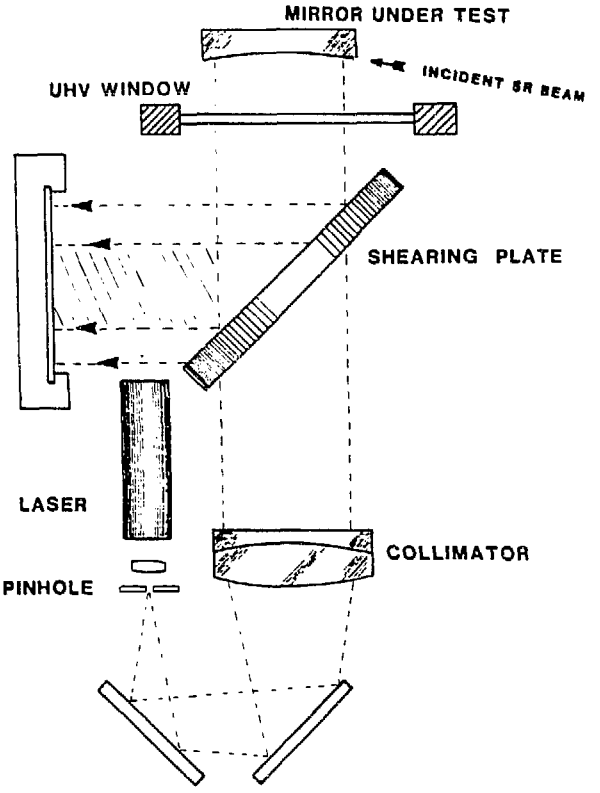

Fig. 3

The experimental arrangement used to make the in situ interferometric measurements. The mirror under test is located in ultra-high vacuum behind a large glass viewport. The laser pinhole source is expanded by the collimator lens, which is slightly defocused to produce a wavefront matching the long radius of the test mirror.

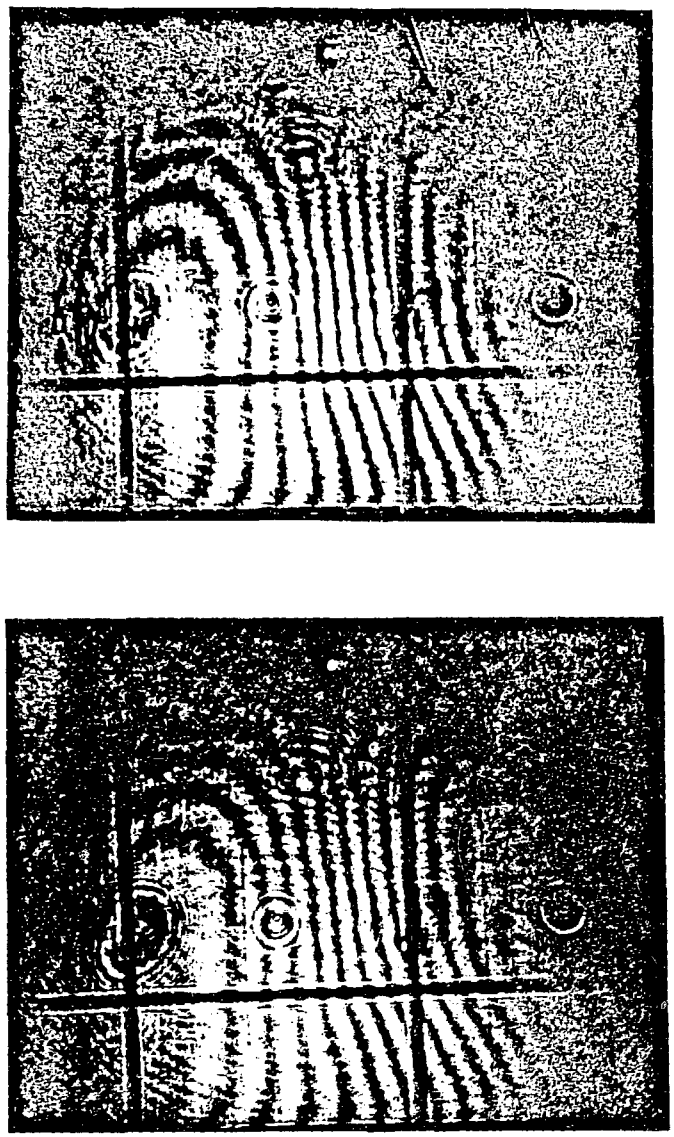

Fig. 4. Interferograms from the X17TA measurements taken at the start and the end of the 3 hour irradiation period. Fiducials on the film plane (not easily seen here) allow one to measure changes in fringe spacing and also the rotational shift of the fringe pattern. These photos indicate that over the 3 hour period the fringe spacing has increased so that 10 fringes at the end of the period (lower frame) occupy the same distance as 10.5 fringes at the start of the time period (upper frame).